FRACTOGRAPHIC ANALYSIS OF AN INTERLAMINAR SHEAR FRACTURE IN A CARBON FIBRE–REINFORCED EPOXY LAMINATE ENHANCED BY CARBON NANOTUBES

M. Kadlec[1*], J. Podzimek[2], J. Siegl[1]

[1]*Czech Technical University in Prague, Faculty of Nuclear Sciences and Physical Engineering, Department of Materials, Trojanova 13, 120 00 Prague, Czech Republic.*
[2]*VZLU - Aerospace Research and Test Establishment, Composite Technologies Department, Beranovych 130, 199 05 Prague, Czech Republic.*
**martin.kadlec@fjfi.cvut.cz*

Keywords: Polymer composites; carbon nanotubes; fractographic analysis; aerospace vehicles

Abstract
Fibre–reinforced polymer composites are successfully used in aerospace industry. Presented paper focuses on a fractographic interpretation of a shear structural fracture in the composite with an epoxy matrix enhanced by carbon nanotubes (CNTs). A shear test was performed to assess an influence of the multi-walled CNTs on the essential mechanical property of the laminated composite – interlaminar shear strength. The shear stress state in specimens during loading and test boundary conditions were verified by a finite element method. Failure mechanisms were determined by means of light and scanning electron microscopy. Fractographic features typical for shear loading were observed. Furthermore, resin aggregates were observed in the specimens enhanced with the CNTs. The aggregates indicate an insufficient distribution of nanotubes in the resin which might cause the non-significant change in the strength obtained in the experiment.

1 Introduction

Polymer composite panels are widely used in the aerospace industry because of their high strength vs. weight ratio. Interlaminar shear strength (ILSS) is an important characteristic required of the composites. The shear strength testing of laminates belongs to the most difficult field of mechanical property testing. Quite many standards were developed to obtain the ILSS value. A short beam shear (SBS) method is the most common test but using this approach, the strength values are only apparent because of the presence of edges, material coupling, non-pure shear loading, non-linear behaviour, imperfect stress distributions and the presence of normal stresses [1]. Therefore, another method was chosen for the experiments. A shear loading test according to DIN standard [2] is able to introduce the shear stress to a specimen in more proper way. The specimens have two slots and they are loaded by tension. This approach brings an advantage of clear and easily accessible fracture surfaces for post failure analyses.

An addition of carbon nanotubes (CNTs) to polymers reinforced with continuous micro-fibres has an effect only on those composite qualities that are controlled by properties of their matrix. The CNTs have been introduced to the composite for several years to improve the

shear strength characteristics. Stiffness, strength and strain to failure in the fibre direction are affected only slightly [3]. The composites with the microscopic reinforcement enhanced by the nano-reinforcements are referred as multiscale, three phase, or nano-engineered fibre–reinforced composites (nFRC).
The authors of reference [4] found out that a polymer matrix with stirred nanotubes has better adhesion to fibres. This was observed using a scanning electron microscope (SEM) for a carbon fibre-reinforced polymer (CFRP) with 1 and 3 weight percent of the nanotubes addition. The nano particles create a new component in the fibre – matrix system which makes the synergic effect more apparent. However, the nanotube walls have very small surface energy which causes problems with creation of bonds with polymer. Creating of nanotube agglomerations which is connected with Van der Walls forces and high length to diameter ratio of nanotubes is another problem which makes the demanding effect difficult to reach. The possible solution is a functionalisation of nanotubes which means a chemical change of the CNT surface. The previous results were promising, e.g. authors in reference [5] were able to increase the ILSS value up to 33%. They used high pressure injection of polymer in preferred normal direction to the weave plane; consequently, the CNTs were aligned in this direction.
A fractographic examination of fracture surfaces enables to deduce information about damage in components. The basic approach entails an understanding of failure mechanisms connected with loading modes. This knowledge can be then used for examination of more complex failures. A variety of fractographic techniques for composites were developed during last 30 years [6, 7]. The making of fractographic atlases like for isotropic material did not succeed because of very high spectrum of failure modes which can interact with each other. Therefore, the specific mechanisms occurring in the constituents need to be understood and applied to the global fracture morphologies [8]. Additional factors like temperature, moisture and loading rate significantly can have an effect on the fracture morphology [6].

2 Experiments and evaluation methods

2.1 Experimental material

Nanotubes were functionalized and introduced to the matrix that their weight percentage reached 0.5% in the resin. The following procedures were performed to achieve this goal. First, the multiwalled CNTs Nanocyl NC7000 with 90% purity were modified for 30 minutes in a solution of inorganic acids. The volume ratio of the sulphuric and nitric acid solution was 3:1. The reaction temperature was 140°C. Second, the mixture was cooled and the CNTs were filtered by 800 nm filter and rinsed in deionised water. Required amount of CNTs was transferred into acetone and inserted into ultrasound bath for 30 minutes. Next, this mixture of CNTs and acetone was stirred with required amount of epoxy resin Araldite LY 5052. The mixing was performed under 60°C and was evacuated for 15 minutes. The reaction was completed by addition of hardener Aradur 5052.
A pair of 4 mm thick plates of a carbon fibre/epoxy unidirectional composite was manufactured using unidirectional carbon weave UD G1157. The fabric was laid up with [0˚]13 stacking sequence for the rectangular plates. The mixture of the resin and the hardener – with added CNTs for one of the two plates – was injected into stacked layers placed in a vacuum bag using 2 bars below the atmospheric pressure (Fig. 1a). The curing was performed under temperature of 50˚C applied for 15 hours.

2.2 Shear test

Test specimens were cut from both the plates, that their length of 200 mm was along the fibre direction. Their width and thickness were 25 mm and 4 mm respectively. Two slots perpendicular to the specimens length were made in a distance of 12.5 mm (Fig. 1b). The slots

depth was from 52 up to 55 % of the specimen thickness. Experimental test procedures were performed on a mechanical loading frame according to DIN 65 148 standard [2]. The loading was carried out using a displacement control with the crosshead moving at a constant rate of 1 mm/min. Since a demanded uniform shear stress field depends on a bending moment, the DIN standard requires a steel fixture which constrains specimen bending. The steel fixture consisted of two plates that are pressed on the both sides of the specimen by 4 screws. The screw force is set so the fixture will not fall due to its own weight. The friction was minimized by fixture polishing. Fig. 1c shows a specimen under loading in the steel test fixture. The failure is intended to occur between the slots where the shear stress intensity has its maximum.

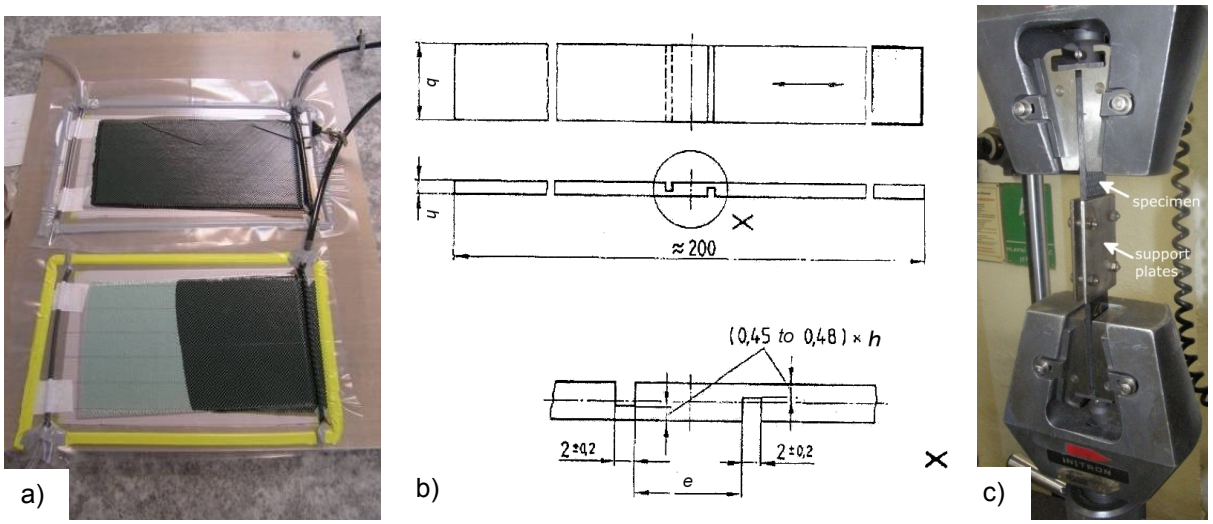

Figure 1. a) Resin transfer into stacked layers of the carbon unidirectional weave placed under a vacuum bag, b) test specimen dimensions and c) the experimental set-up arrangement.

The interlaminar shear strength is defined as:

$$\tau_s = P/(be), \tag{1}$$

where P is the maximal applied load, b is the width of the specimen and e is the distance between the slots.

2.3 FEM

The tensile test of the slotted specimens was simulated by a finite element method (FEM). This analysis was performed to verify the required uniform distribution of the shear stress field. A two-dimensional model 100 mm long was made in the ABAQUS software [11]. This model was divided into linear shell planar elements of the type CPE4R with the default hourglass control. The element size approximately corresponded to 0.4 mm in the area with the stress concentration. The layered structure of the composite was not considered. The modelled material was orthotropic with parameters typical for CFRP T300/5208 laminate: E_x = 181 GPa; E_y = 10,3 GPa; μ_{xy} = 0,28; G_{xy} = 7,17 GPa, where x corresponds to the length and y to the thickness of the specimen. These parameters were adopted from ref. [12].The applied force of 25 kN on the border elements corresponded to 80 MPa shear stress in the middle plane. The influence of the constrained conditions using the supporting fixture was evaluated by applied contact surfaces without friction. Both the surface to surface contacts were set to normal behaviour with default constrained enforcement method by “hard” contact. After a load being applied to the model, the fixture model was approached to the specimen.

2.4 Failure mechanisms

The fibre fracture and the inter-fibre (matrix) fracture are the two main groups of failure modes [13]. In addition, according to a fracture location in a laminate, three classes can be defined [9] as translaminar, interlaminar and intralaminar fracture: The translaminar fracture is entails failure of fibres occurring typically under tension and compression stress. The intralaminar fracture means failure of matrix within a ply or a fibre tow. Its most typical feature is a fibre tow splitting appearing in the transverse direction to loading. The interlaminar fracture entails failure of the matrix between layers also known as a delamination. The delamination differs from the other modes by greater fracture area since a crack between the layers is not inhibited.

The major failure mode during shear loading is the matrix fracture. Specific fractographic features for shear loaded delaminated fractures are cusps which appear as inclined platelets on the surface perpendicular to the loading [9]. Other resin features can be gouges and riverlines. The riverlines can occur between the fibres in the resin rich areas and the local crack growth direction can be determined by them.

Basic failure mechanism		**fracture features**
fibre fracture	**trans**laminar	fibre cleavage, microbuckling, kinkbands
inter-fibre fracture	**intra**laminar	bundle crack (ply splitting), micro-delamination, fibre bridging
	interlaminar	delamination, matrix cleavage, cusps, gouges, riverlines

Table 1. Failure mechanisms according to references [3, 9, 13]

3 Results and discussion

3.1 Analysis of the experimental design

The shear tests were performed at room temperature on 15 specimens out of which 5 had enhanced matrix with the nanotubes. Table 2 shows the maximum force and strength values for all the specimens. An outlier criterion for single samples showed no outliers for either of the groups and the Lilliefors test did not rejected the normality of the groups. The arithmetic means are different and the nano-enhanced specimens have lower value by 2.4 MPa (Fig. 4). However, the standard deviation is approximately 4 MPa for both groups. Therefore, the statistical t-test was performed with the result of $p = 0.28$ which means that the difference in shear strengths for the groups is not significant at $\alpha = 0.05$ significance level.

Neat matrix			***Nano-enhanced matrix***		
spec. label	F_{max} **(N)**	τ_s **(MPa)**	**spec. label**	F_{max} **(N)**	τ_s **(MPa)**
Mean	7025	**22.2**	**Mean**	6287	**19.8**
s_{n-1}	1174	**3.7**	s_{n-1}	1209	**3.8**

Table 2. Experimental results of interlaminar shear strength τs values measured on 2 groups of specimens.

3.2 Shear strain contours

A full field shear strain distribution for the slotted specimen under tensile load was calculated by FEM and is shown in Fig. 2. The calculated strain values in the middle section were exported for both the fixture supported and the unsupported specimen. Both the section curves and an ideal stress value from equation (1) are visible in Fig. 3. Without the supports, there is a high concentration of stress near the slots and an insufficient shear stress in the middle plane. With the supports, the values do not exceed the predicted values and the shear stress field is consistent with eq. (1). The maximum shear stress deviation is 20 %, in between the slots.

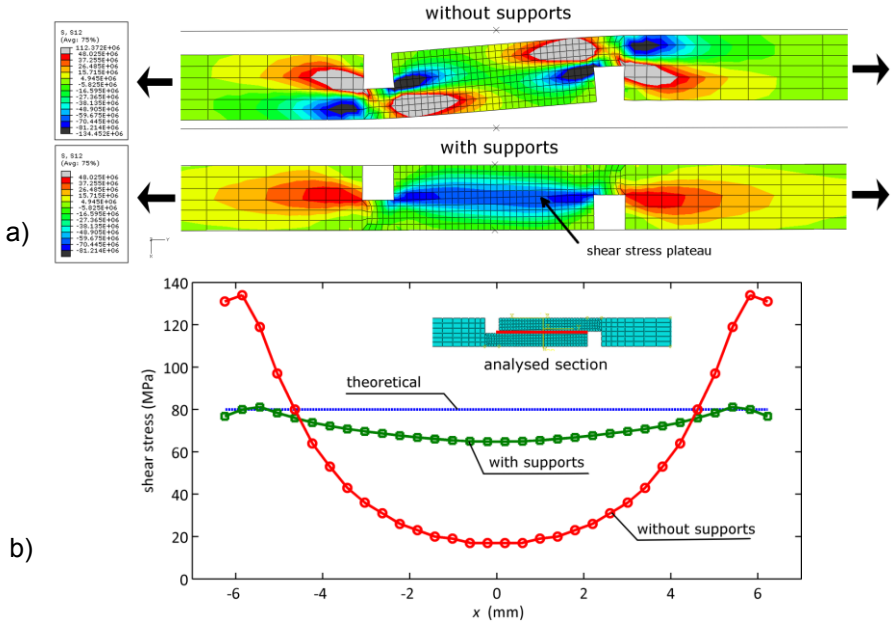

Figure 2. a) Shear strain τ_{xz} measurement contours overlay of the specimen during tensile loading of a free and a supported specimen, b) Shear strain curves in the middle plane section between the slots. The results indicate the strong influence of various boundary conditions and show a comparison with the theoretical values (eq. (1)).

3.3 Fractographic analyses

At first, a fractographic analysis from the macroscopic point of view was performed. The specimens had a unidirectional plain weave with 96 wt.% of carbon fibres in the warp direction and 4 wt.% of glass fibres in the weft direction. Four specimens were chosen for the detailed fractographic analysis. Two specimens C3 and C7 from the non-enhanced group and specimens CN2 and CN4 form nano-enhanced group. The selection was made in order to evaluate the specimens with both the minimum and maximum strength. The specimens fracture occurred in accordance with the DIN standard, i.e. the fibres were not pulled-out because of inappropriate cut depth.

The observed failure mechanisms were a combination of interlaminar (delamination) and intralaminar failure (Fig. 3). The delaminated surface has apparent weave pattern with weft glass fibres imprinted to the opposite face. The intralaminar failure can be identified by a rough surface with pulled fibre tows and damaged weft glass yarns. The mentioned failure modes were observed independently without any reliance on the nanotubes enhancement. Apparently, the resulting fracture morphology depends on the relative position of the tows and the slot bottom.

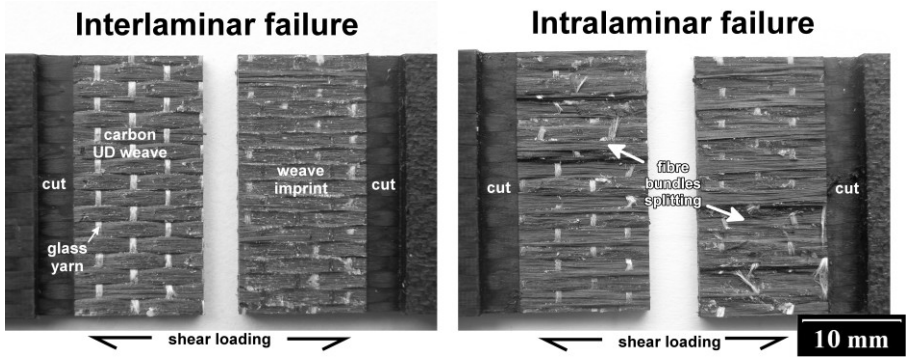

Figure 3. Matching faces of a shear-mode fracture of two CFRP specimens with observed a) Interlaminar failure of specimen C5 and b) intralaminar failure of specimen C10. Other specimen failed by a combination of these failure mechanisms.

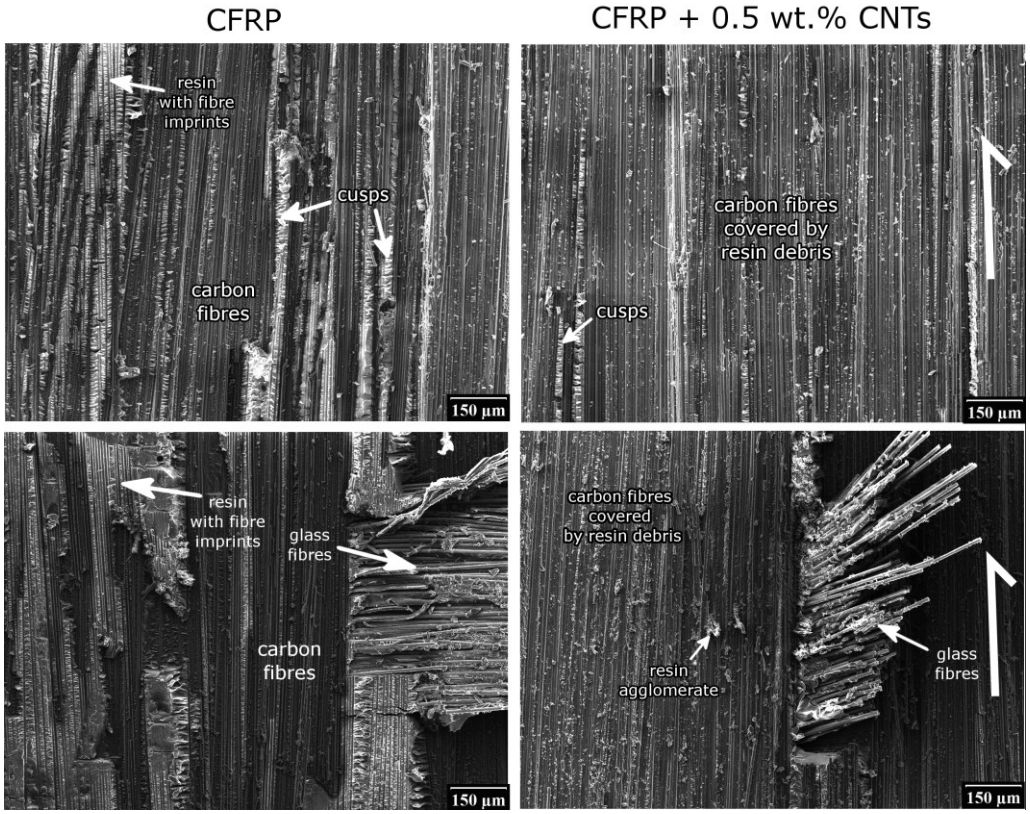

Figure 4. Fracture surfaces of the CFRP laminate observed using SEM. Cusps typical of shear loading and fibre imprints were observed in the neat resin (C3, C7) and also in nano-enhanced (CN2, CN4) specimens. More resin debris and resin agglomerates were apparent on nano-enhanced specimens shown in the second column.

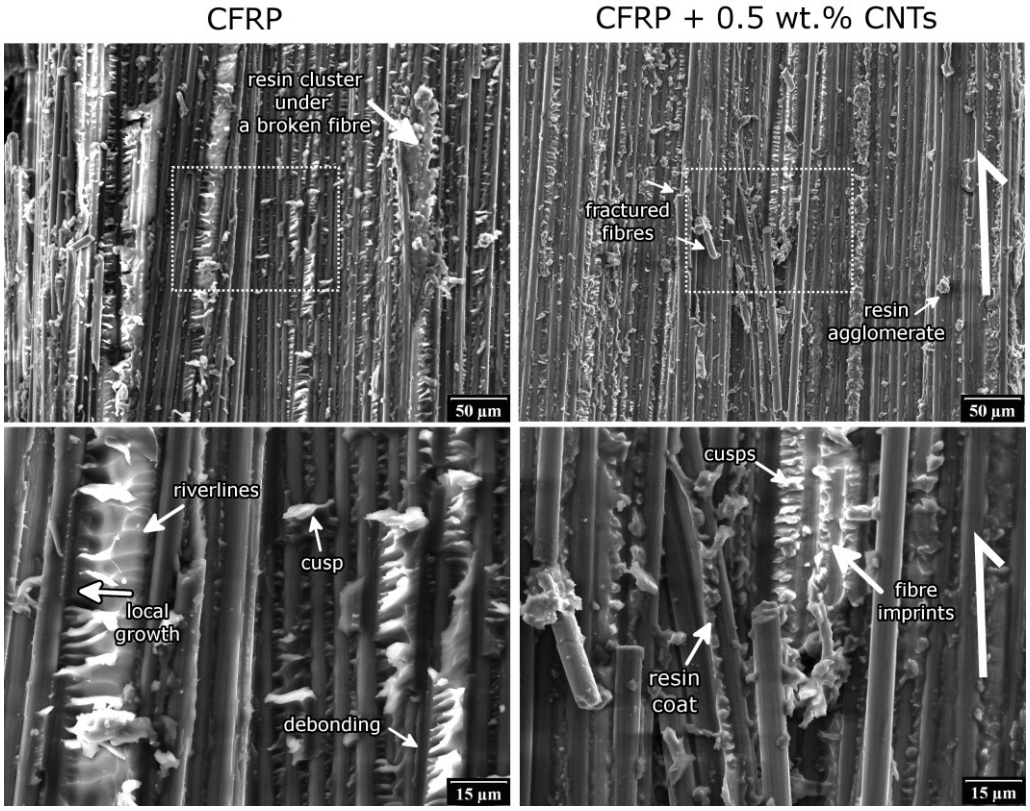

Figure 5. Fracture surfaces of the CFRP laminate observed using the SEM. A few broken fibres were observed on both the specimens. Riverlines with marked local crack growth were visible. Resin agglomerates and resin coating on fibres were observed in the nano-enhanced specimens.

The fractographic analysis from the microscopic point of view was performed using the scanning electron microscope JSM 5510LV in the secondary electron regime under 10 kV acceleration voltage. The fracture surfaces were observed by magnifications of 100x up to 10 000x. This analysis was performed to assess the fractographic features typical of the interlaminar mechanism and an effect of nanotubes presence in the matrix of the tested specimens. The specimens were not metalized because the carbon fibres were able to transfer the electrons off of the specimen. Considering the fact that the unidirectional laminate has high anisotropy for electric current, the electron transfer was directed by a conductible paste applied to the specimen sidewall that was in the normal direction to the fibres.

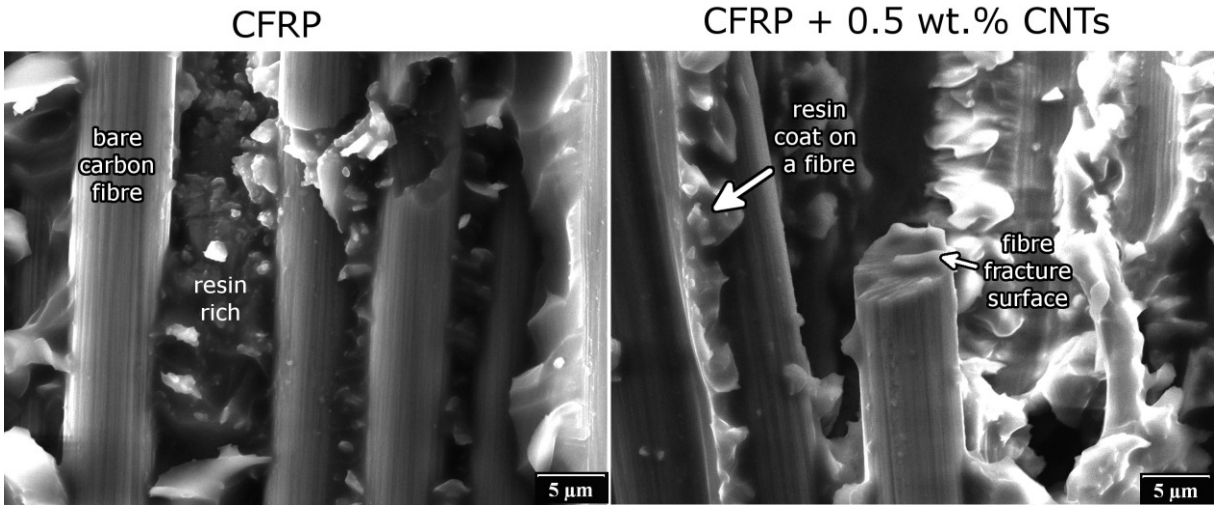

Figure 6. Fracture surfaces of the CFRP laminate observed using SEM. Bare carbon fibre and a resin rich area were observed on the C3 specimen. Resin coat on a fibre a fibre cleavage was observed on the specimen CN4 enhanced by nanotubes.

Following micromorphologic characteristics were found on all the observed specimens (Figures 4, 5 and 6). Dark areas of bare carbon fibres and bright areas of a resin with fibre imprints were visible. Cusps typical of the shear loading were found during more detailed analysis of the resin. Riverlines in the resin typical of isotropic materials were also found. The local crack growth direction could be stated in perpendicular direction to the macroscopic loading. Glass fibres were coated by the resin more than the carbon fibres. A minor observation of broken carbon fibres was documented and a fibre cleavage was observed.
The following morphological features were visible more often in the nano-enhanced specimens. Resin debris covering the fracture surface and even some bigger resin agglomerates were apparent. More detailed analysis showed a resin coating of the carbon fibres. The resin coating and the debris show improved matrix-fibre boundary strength.

4 Discussion and conclusion

This study evaluated possible influences of carbon nanotubes (CNTs) stirred in the resin of carbon fibre-reinforced polymer laminates. The unidirectional laminates were tested by shear loading.

- An influence of the supporting fixture was calculated using FEM. Without the supports, there is a high concentration of stress near the slots and an insufficient shear stress in the middle plane. With the supports, the values do not exceed the predicted values and the shear stress field is consistent with the used equation for strength evaluation.
- The effect of CNTs on the strength values was not statistically significant because of the high deviation of strength values obtained using the DIN method.

- The macroscopic analysis showed two fracture modes. The Interlaminar and intralaminar fractures were observed independently of the nanotubes presence. No correlation of the strength values and the fracture modes was found. A relative position of the slot depth and a ply boundary had apparently an effect on the fracture mode.
- The fractographic evaluation using SEM showed some differences in the nano-enhanced specimens. It revealed resin coating and agglomerates in the nano-enhanced specimens. More resin debris was found on these specimens as well. Typical features of shear loading like cusps were perceived. Riverlines typical of isotropic materials were found in some resin rich areas.

Acknowledgments
The experiments carried out in the VZLU were supported by institutional funding from the Ministry of Industry and Trade of the Czech Republic. The fractographic analyses were realized by the Czech Technical University in Prague in the frame of the project SGS 10/301/OHK4/3T/14.

References

[1] *Composite Materials Handbook – Volume 1. Polymer Matrix Composites, Guidelines for Characterization of Structural Materials* [online]. Department of Defense, Fort Washington (2002). URL: <http://www.acm-nevada.com/Technical/HDBK17-1F.pdf>.
[2] DIN 65 148. *Bestimmung der interlaminaren scherfestigkeit im zugversuch* (1986).
[3] De Greef N., et al. Damage development in woven carbon fiber/epoxy composites modified with carbon nanotubes under tension in the bias direction. *Composites Part A: Applied Science and Manufacturing*, **vol. 42**, pp. 1635-1644 (2011).
[4] Palmeri M.J., et al. Multi-scale reinforcement of CFRPs using carbon nanofibers. *Composites science and technology*, **vol. 71**, pp. 79-86 (2011).
[5] Fan, Z., Santare M.H., Advani S.G. Interlaminar shear strength of glass fiber reinforced epoxy composites enhanced with multi-walled carbon nanotubes. *Composites Part A: Applied Science and Manufacturing*, **vol. 39**, pp. 540-554 (2008).
[6] Roulin-Moloney A.C. *Fractography and failure mechanisms of polymers and composites*. 1st ed. Elsevier Applied Science, University of Michigan (1989).
[7] Purslow D. Some fundamental aspects of composites fractography. *Composites*, vol. 12, pp. 241-247 (1981).
[8] Greenhalgh E.S., Hiley M.J. *Fractography of polymer composites: current status and future issues* in "Proceedings of the *13th European conference on composite materials (ECCM13)*". KTH Royal Institute of Technology, Stockholm (2008).
[9] Greengalgh E.S.: *Failure Analysis and Fractography of Polymer Composites*. 1st ed. Woodhead Publishing, Cambridge (2009).
[10] Friedrich K. *Application of Fracture Mechanics to Composite Materials*. Elsevier Science, Amsterdam (1989).
[11] *Abaqus/CAE*. Version 6.9. Dassault Systèmes, Vélizy-Villacoublay, France (2009).
[12] Yang C. *Analytical Modeling of ASTM Lap Shear Adhesive Specimens*. Wichita State University, Wichita (2003).
[13] Ehrenstein G.W. *Polymerní kompozitní materiály*. Scientia, Prague (2009).